Vacuum-UV negative photoion spectroscopy of SF5CF3

Simpson, M. J.; Tuckett, R. P.; Hunniford, C. A.; Scully, S. W. J.; Dunn, KF; Latimer, CJ

DOI:
10.1063/1.2894869

M.J. Simpson, R.P. Tuckett, K. Dunn, A. Hunniford, C.J. Latimer and S.W.J. Scully

Vacuum-UV negative photoion spectroscopy of SF_5CF_3

J. Chem. Phys., (2008) **128 (12),** 124315-1 – 124315-10

DOI: 10.1063/1.2894869

Professor Richard Tuckett (University of Birmingham) / July 2011

A8.01.087 *Manuscript to AIP following acceptance by JCP office* *February 18, 2008*
AIP ID : 010813JCP

Vacuum-UV negative photoion spectroscopy of SF_5CF_3

M. J. Simpson and R. P. Tuckett,*

School of Chemistry, University of Birmingham, Edgbaston, Birmingham B15 2TT, United Kingdom

K. F. Dunn, C. A. Hunniford, C. J. Latimer and S. W. J. Scully

Department of Physics and Astronomy, Queen's University Belfast, Belfast BT7 1NN, United Kingdom

Number of pages : 22 (excluding tables and figure captions)
Number of tables : 2
Number of figures : 5

* Author for correspondence, tel +44 121 414 4425, fax +44 121 414 4403, email r.p.tuckett@bham.ac.uk

---

Ion pair formation, generically described as $AB \rightarrow A^+ + B^-$, from vacuum-UV photoexcitation of trifluoromethyl sulfur pentafluoride, SF_5CF_3, has been studied by anion mass spectrometry using synchrotron radiation in the photon energy range 10–35 eV. The anions F^-, F_2^- and SF_x^- (x = 1–5) are observed. With the exception of SF_5^-, the anions observed show a linear dependence of signal with pressure, showing that they arise from ion pair formation. SF_5^- arises from dissociative electron attachment, following photoionization of SF_5CF_3 as the source of low-energy electrons. Cross sections for anion production are put on to an absolute scale by calibration of the signal strengths with those of F^- from both SF_6 and CF_4. Quantum yields for anion production from SF_5CF_3, spanning the range 10^{-7} to 10^{-4}, are obtained using vacuum-UV absorption cross sections. Unlike SF_6 and CF_4, the quantum yield for F^- production from SF_5CF_3 increases above the onset of photoionization.

I. INTRODUCTION

The presence of the super greenhouse gas trifluoromethyl sulfur pentafluoride, SF_5CF_3, in the atmosphere was first reported in 2000 by Sturges *et al*.[1] Although the known atmospheric concentrations of SF_5CF_3 are very low, its lifetime is in the region of 1000 years,[2] and it is thought to have a Global Warming Potential 18,000 times greater than CO_2, absorbing strongly in the infrared between 750 and 1250 cm^{-1} (Ref. 3). Of anthropogenic origin, SF_5CF_3 has been linked to SF_6 production and the manufacture of fluorochemicals,[1] but in truth the main source of this potent greenhouse gas has not yet unambiguously been identified. Since its discovery, SF_5CF_3 has been the focus of numerous studies aimed to understand better its spectroscopic properties and reactivity. Laboratory experiments have confirmed the original estimates on the severity of SF_5CF_3 as a greenhouse gas,[3-6] yet more work is required to gather a more comprehensive understanding of its sources and sinks. The original suggestion that SF_5 and CF_3 radicals combine to produce SF_5CF_3 in high voltage equipment[1] has since been disputed;[7] reactions mimicking these conditions showed no evidence of SF_5CF_3 production, although small amounts were detected when SF_6 reacted with some hydrofluorocarbons in a spark discharge.[7] Low energy electron attachment to SF_5CF_3 is dissociative[8-12] and may provide a mechanism for atmospheric removal, but stratospheric UV photolysis is unlikely to contribute due to the absence of photoabsorption by SF_5CF_3 below 8 eV[4] and the high value of the SF_5–CF_3 bond dissociation energy (4.06 ± 0.45 eV at 0 K).[13,14] Following a new measurement of the ionization energy of the CF_3 radical,[15] this bond strength has since been refined to 3.86 ± 0.45 eV.[16]

The surprisingly high value of the S–C bond has spurred investigations into the sink routes for SF_5CF_3 that might occur at higher altitudes in the mesosphere or ionosphere: ion-molecule reactions, electron attachment, and vacuum-UV (VUV) photodissociation at the Lyman-α wavelength of 121.6 nm. Ion-molecule reaction studies have shown that both cations[17,18] and anions[19] react rapidly with SF_5CF_3 and may therefore remove it from the mesosphere / ionosphere. However, the concentration of atmospherically-relevant ions (*e.g.* O^+, O_2^+, N^+, N_2^+) is so low that the pseudo-first-order rate constant for ion-molecule reactions, $\sum k_{ion}[\text{ion}]$, is too

small for this channel to contribute to any significant extent.[16] Low-energy electron attachment to SF_5CF_3 is relatively fast, 7.7 x 10^{-8} cm^3 $molecule^{-1}$ s^{-1} at 298 K,[8] and the absorption cross section at 121.6 nm is surprisingly high, *ca.* 10^{-17} cm^2 (Refs. 2, 20). By comparison with equivalent data for SF_6, it was shown that the electron attachment process is responsible for ~99% of the removal of SF_5CF_3 in the mesosphere, VUV photodissociation ~1%.[2] However, the long lifetime of SF_5CF_3 in the earth's atmosphere, ~1000 years, is not determined by these *microscopic* chemical processes that occur in the mesosphere, but by the much slower *macroscopic* meteorology that transports the pollutant from the earth's surface up into the mesosphere.[2] Advances made in the last six years to understand the chemical physics properties and environmental impact of SF_5CF_3 since its discovery in 2000 have been reviewed.[16]

One of the possible products following VUV photoexcitation of SF_5CF_3 at 121.6 nm is ion-pair formation, *e.g.* $CF_3^+ + SF_5^-$ (Ref. 2). In this paper we describe an experiment to detect anions following VUV excitation as a means to study the dynamics of electronically excited states of SF_5CF_3. Absolute cross sections for anion production and, using photoabsorption data,[20] quantum yields have been evaluated for all the anion products observed. Photoion pair formation has been observed from many diatomic and small polyatomic molecules since the 1930s.[21] Ion pair states are reached either by direct photoabsorption, or *via* predissociation following photoexcitation to an excited electronic state (which is usually Rydberg in character).[21,22] Based on Frank-Condon arguments, the latter process is thought to be more common, although significant coupling between Rydberg and ion pair states is a requirement – one which is not always met. The study of ion pair formation, therefore, can provide insight into the initial processes involved before the positive-negative pair of ions evolves, *i.e.* the decay dynamics of Rydberg states. Above the ionization energy (IE) of the parent neutral molecule, photoionization dominates and quantum yields for ion pair formation, Φ_{IP}, are expected to be low, typically less than 10^{-3}. Even below the IE, for polyatomic molecules Φ_{IP} is typically only ~10^{-2} (Ref. 22). A recent ion pair study on CH_3Cl, CH_3Br and CF_2Cl_2, aiming specifically at the photon energy region below the IE of the parent neutral, has highlighted the significance of

predissociation into a state yielding neutral fragments rather than one yielding ion pairs.[23] In addition to SF_5CF_3, the closely-related molecules SF_6 and CF_4 have also been investigated in this paper. The photoion pair formation of SF_6 into $SF_5^+ + F^-$ and CF_4 into $CF_3^+ + F^-$ has been studied previously by Mitsuke *et al*.[24,25] and Scully *et al*.[26] We have seen a much larger number of anions than observed by these groups, and the data of Mitsuke *et al*.[24,25] has allowed us to put our SF_5CF_3 data on an *absolute* scale. To our knowledge this is the first report of ion pair production following VUV photoexcitation of SF_5CF_3.

II. EXPERIMENTAL

Beamline 3.1 at the UK Daresbury synchrotron radiation source (SRS) is optimised for high flux in the VUV,[27] and a 1 m Wadsworth monochromator provided the source of tunable radiation (~ 8–35 eV) used for this experiment. The optimum resolution of this beamline is 0.05 nm, or 0.016 eV at 20 eV. A 2 mm diameter, 300 mm long capillary light guide connecting the experimental apparatus to the beamline focuses monochromatized light directly to the interaction region. The ion pair apparatus has been described in detail elsewhere.[28] Briefly, the gas under study is injected *via* a needle generating a directed jet which bisects orthogonally the incident photon beam. The crossing point, which dictates the centre of the interaction region, is positioned in the middle of two grids on the third orthogonal axis. A potential difference across the grids sweeps negative ions along this axis towards a 3-element electrostatic lens for focusing, and into a Hiden Analytical HAL IV triple quadrupole mass spectrometer (QMS) for mass selection. Detection is achieved by a channeltron electron multiplier. Sensitivity is considerably enhanced by differential pumping which reduces the number of free electrons and secondary collisions in the QMS. Spectra in which the monochromator is scanned are flux normalized using a sodium salicylate window and visible photomultiplier tube (EMI 9924B) combination, which has a constant response over the energy range of the experiments. The apparatus and QMS, connected *via* a 1 mm diameter aperture, are pumped separately by turbo pumps which are backed by a common rotary pump, and the base pressure of the apparatus is $\sim 10^{-7}$ mbar. With sample gas running, the typical pressure in the chamber is $\sim 10^{-5}$ mbar. The pressure inside the chamber was

measured using an ionization gauge, the sensitivity of which to SF_6, CF_4 and SF_5CF_3 is calibrated in a separate experiment relative to N_2 gas using a capacitance manometer.

Mass spectra are recorded to observe all anions produced from photoabsorption of the sample gas by exposure to white light, *i.e.* a wavelength of 0 nm. The mass-to-charge ratio (*m/z*) of each peak in the mass spectrum is then fixed and the signal recorded as a function of sample gas pressure over the typical range $(0.5–5.0) \times 10^{-5}$ mbar. Anions which show a non-linear dependence with pressure cannot be assigned as ion pair products, and their signal is most likely influenced by secondary processes. Anions which show a linear dependence of signal with pressure can be attributed to ion pair formation. For all anions produced from SF_6, CF_4 and SF_5CF_3, ion yields were recorded as a function of photon energy from 8–35 eV. Two gratings span this range, the higher-energy grating covering 12–35 eV. The majority of experiments were performed with this grating. The lower-energy grating covers the range 8–18 eV, and for scans below 11.8 eV (or 105 nm) a LiF window can be inserted to eliminate higher-order radiation. This grating was used in one scan to record the threshold region of F^- from SF_5CF_3. Gas samples were obtained from Apollo Scientific with a quoted purity of > 99.9%, and were used without further purification.

The ion yields are presented as anion cross sections, σ, in units of cm^2. The value of σ at photon energy hν is given by:

$$\sigma(h\nu) = k\left(\frac{S \times m}{f \times r \times p}\right) \qquad (1)$$

S is the detected signal in counts s^{-1}, *f* the relative photon flux, *p* the sample gas pressure adjusted for ionization gauge sensitivity, *r* the storage ring current, *m* the relative mass sensitivity of the quadrupole, and *k* a normalization constant. Thus the signal strength is normalized to photon flux, pressure, ring current and mass sensitivity of the quadrupole. The relative photon flux as a function of hν is measured in a separate

experiment with no sample gas present, so it is necessary to correct *S* both for *f and r*. The value of *m* as a function of mass in the range 19–127 u (*i.e.* F^- to SF_5^-) is derived from a comparison of the cation spectrum produced by 70 eV electron impact ionization of the sample gas (with the photon beam blocked) with that published elsewhere.[29] Like most quadrupoles, the sensitivity of our mass spectrometer decreases with increasing mass of the ion; *m*, as defined in Eq. (1), therefore increases with increasing mass. The corrected signal for F^- from SF_6 is then normalized to the known cross section at 14.3 eV, $(7 \pm 2) \times 10^{-21}$ cm^2 (Ref. 24). Likewise, the corrected signal for F^- from CF_4 is normalized to its value at 13.9 eV, $(1.25 \pm 0.25) \times 10^{-21}$ cm^2 (Ref. 25). [It is noted that these cross section values are not strictly absolute, but are obtained from calibrated measurements of O^- yields from O_2 (Ref. 30)]. In theory, the values k (F^-/SF_6) and k (F^-/CF_4) should then be equal, but in fact they differ by a factor of 1.6. Given the number of corrections made to the anion signals, this difference seems a reasonable representation of experimental error. An average of the two k values is then used in Eq. (1) to determine absolute cross sections for the SF_5CF_3 anion signals. We comment that, whilst these values of anion cross sections probably have an error as high as ± 50–100 %, such *absolute* measurements are notoriously difficult and prone to errors which are often underestimated in the literature. Scully *et al*.[26] estimated the cross section for the F^- peak from SF_6 at 24.6 eV to be $2.0 \pm 0.5 \times 10^{-21}$ cm^2, and this value agrees within experimental error with our value of 1.6×10^{-21} cm^2. Likewise, Scully[31] estimated the cross section for F^- production from CF_4 at 21.8 eV to be $5 \pm 1 \times 10^{-22}$ cm^2, again agreeing reasonably well with our value of 6.7×10^{-22} cm^2. This confirms that our method of determining absolute cross sections by normalizing the signal at one energy is applicable across the complete energy range of the experiment, *ca.* 10–25 eV. We believe it is therefore appropriate to present *all* the anion yields as absolute cross sections.

III. THERMOCHEMISTRY: GENERAL COMMENTS

Our work also determines appearance energies (AE) at 298 K for many fragment anions from SF_5CF_3, CF_4 and SF_6, and we compare these values with those calculated from thermochemical data. Berkowitz[21] has

noted that, for many polyatomic molecules, a calculated threshold energy provided a lower limit to the experimental AE of an anion when suitable assumptions were made about the nature of the accompanying cation and / or neutral fragments. However, usually there was equality in these two values, although it is noted that *energy* and *enthalpy* are often indistinguishable words. In making comparisons between our experimental AE values of anions and calculated enthalpies of appropriate dissociation reactions, we make two assumptions which we believe are justified at the relatively modest resolution of our experiment, *ca.* 0.1–0.2 eV. First, it is now well established that it is not accurate to equate an AE_{298} to the enthalpy of the corresponding unimolecular reaction at 298 K because of thermal effects.[32] In practice, the corrections needed to the AE_{298} values are typically only 0.05–0.15 eV, and we feel justified in ignoring them. Second, the effects of entropy are disregarded in our calculations, even though many of the unimolecular reactions involve a value for $\Delta n > 0$, where Δn is the number of product species minus the number of reactant species. Thus $\Delta_r S^o_{298}$ will be positive, and $\Delta_r G^o_{298}$ for the unimolecular reactions will be more negative than the calculated $\Delta_r H^o_{298}$ values. Finally, we should note that many of the values of enthalpies of fomation, $\Delta_f H^o_{298}$, for polyatomic fragments from SF_5CF_3 (*e.g.* SF_4CF_3, $SF_3CF_3^+$) are not known, and this places a severe limitation on the extent to which we can interpret the AE values for anions produced from SF_5CF_3. Even for SF_6, there is still uncertainty in values for $\Delta_r H^o_{298}$ of the $SF_x^{(+)}$ species (x = 3–5). Data for fragments of CF_4 are better established.

IV. RESULTS AND DISCUSSION

A. SF_6

The white light negative ion mass spectrum for SF_6 shows eight peaks corresponding to the anions F^- (100%), F_2^- (1%), SF^- (<1%), SF_2^- (<1%), SF_3^- (<1%), SF_4^- (<1%), SF_5^- (2%), and SF_6^- (67%). The relative signal strengths are shown in parentheses. All anion signals from SF_6 recorded as a function of photon energy are presented in Figure 1, whilst Table I shows AE values of the anions, their cross sections and quantum yields. For comparative purposes, Figure 1 includes the threshold photoelectron spectrum

(TPES) of SF_6.[33] Poor signal strengths prevented ion yields for SF^-, SF_2^-, SF_3^-, and SF_4^- from being recorded. The F^- and F_2^- signals increase linearly with pressure, those of SF_5^- and SF_6^- non-linearly with the rate of change increasing as pressure increases (Figure 2).

Previous ion pair experiments have also observed SF_5^- and SF_6^- from SF_6, their formation being attributed to electron attachment processes:[24,26]

$$SF_6 + h\nu \rightarrow SF_6^+ + e^- \quad (2)$$

$$SF_6 + e^- \rightarrow SF_6^- \quad (3)$$

$$SF_6 + e^- \rightarrow SF_5^- + F \quad (4)$$

There can be little argument that reaction (3) must be responsible for the appearance of SF_6^-, and certainly SF_6 is a well-known electron scavenger, the rate coefficient at 300 *K* being $2.38 \pm 0.15 \times 10^{-7}$ cm^3 s^{-1} (Ref. 11), which attaches zero-energy electrons with a very large cross section.[36] Furthermore, Figure 1 highlights the striking similarities between the SF_6^- spectrum and the SF_6 TPES. The only significant difference between the two is the peak at 19.9 eV, which appears stronger in the SF_6^- spectrum. The same comparison has been discussed by Yencha *et al*.[34] who compared their TPES of SF_6 with the ion yield of SF_6^- produced from SF_6 reported by Mitsuke *et al*.[24]; the same discrepancy in relative signal strengths between the bands at 19.9 eV was observed. We note that the cross section for non-dissociative electron attachment to SF_6 peaks at very low energy characteristic of *s*-wave capture,[36] but SF_6^- anions observed from reaction (3) will arise from *all* electrons integrated under the σ *vs.* electron energy distribution. By contrast, the TPES arises only from low-energy electrons detected within the bandpass of the threshold analyser, *ca.* 4 meV.[33] In practice, the experimentally-observed resolution will depend upon a convolution of the electron energy distribution and the resolution of the photon source. In both experiments the monochromator resolution, *ca.* 0.4 nm or 130 meV at 19.9 eV, will probably dominate. Notwithstanding this point, there is no reason why the

intensities of the TPES and SF_6^- spectra in Figure 1 should be *exactly* the same, and this may explain the small differences that have been observed both by us and by Yencha *et al*.[34] We also note that this difference may not be a particular property of SF_6, because a similar inconsistency in intensities in the threshold photoelectron and parent anion yields has been observed with another polyatomic molecule which attaches electron very rapidly, *cyclic*-C_5F_8.[37] There are two observations from our work which provide evidence for SF_5^- arising predominantly from reaction (4). First, the SF_5^- signal increases non-linearly when recorded as a function of pressure, consistent with the two-step mechanism represented by reactions (2) and (4); an anion signal arising from ion pair formation, $SF_6 + h\nu \rightarrow F^+ + SF_5^-$, would increase linearly with pressure. This is illustrated in Figure 2 which shows clearly the contrast between the signal for the ion pair product, F^-, and that for SF_5^-. Second, the SF_5^- ion yield shows many similarities to the TPES of SF_6 whereas that of F^- does not. However, these arguments do not exclude the possibility that a small amount of SF_5^- is produced *via* the ion pair reaction above.

The F^- and F_2^- signals both increase linearly with pressure, and the following ion pair reactions are suggested as mechanisms for their formation:

$$SF_6 + h\nu \rightarrow SF_6^* \rightarrow F^- + SF_x^+ + (5 - x)\,F \qquad (x \leq 5) \qquad (5)$$

$$SF_6 + h\nu \rightarrow SF_6^* \rightarrow F_2^- + SF_x^+ + (4 - x)\,F \qquad (x \leq 4) \qquad (6)$$

Using enthalpies of formation at 298 *K* for F^- of –249 kJ mol^{-1} (Refs. 38, 39), F_2^- of –301 kJ mol^{-1} (Ref. 40) and SF_x^+ given elsewhere,[41] the calculated enthalpies of reaction for (5) are 10.4, 15.0, 15.5, 19.6 and 23.7 eV for x = 5–1, respectively. For reaction (6) they are 13.5, 13.8, 18.3 and 22.4 eV for x = 4–1, respectively. F^- produced from reaction (5) has been observed before in the photon energy range 11–31 eV and a detailed analysis performed.[24] Below 15.0 eV the associated cation can only be SF_5^+, and the present work (Figure 1) is in very good agreement with this earlier study. Scully *et al.* have observed the ion pair products F^- and F_2^-

from SF_6 in the photon energy range 20–205 eV.[26] Both fragment ions show broad bands centered at 35.5 eV. Although not photoexciting SF_6 above 35 eV, our study clearly shows the onsets for these features.

The F_2^- spectrum in Figure 1 shows features in the photon energy range 16–21 eV which have not been observed before. Below 18.3 eV it is not possible to say whether the associated cation is SF_4^+ or $SF_3^+ + F$. The low F_2^- cross section is reflected in its low signal strength, resulting in a poor signal-to-noise ratio. We identify three peaks centered at 17.2, 18.2, and 19.7 eV. They most likely reflect the presence of Rydberg states which couple effectively to the ion pair state, the peak energies therefore representing Rydberg transitions. Mitsuke *et al.* found that the most prominent features in the F^- ion yield at 13.2 and 14.3 eV were due to Rydberg transitions.[24] The peaks in the F_2^- ion yield at 17.2, 18.2, and 19.7 eV approximately match with peaks in the TPES of SF_6 at 17.1, 18.5, and 19.9 eV, respectively. A similar observation is made in the F_2^- ion yield from SF_5CF_3 (Section C. III.).

B. CF_4

The white light negative ion mass spectrum for CF_4 shows three peaks corresponding to the anions F^- (100%), CF^- (1%) and F_2^- (3%). The F^- and F_2^- signals were recorded as a function of photon energy and are shown in Figures 3(a) and 3(b), along with the TPES of CF_4 [(Ref. 33), Figure 3(e)] which is included for comparative purposes. The corresponding data is shown in Table I. The CF^- signal rises non-linearly with pressure but, unlike SF_5^- from SF_6 (Figure 2), the rate of increase of signal with pressure *decreases* as the pressure increases. The CF^- signal must therefore be affected by a significant CF^- removal process. The ion yield of CF^- was not obtained due to the poor signal strength.

The F^- and F_2^- signals both increase linearly with pressure and the following ion pair reactions are suggested as mechanisms for their formation:

$$CF_4 + h\nu \rightarrow CF_4^* \rightarrow F^- + CF_x^+ + (3 - x)\,F \qquad (x \leq 3) \qquad (7)$$

$$CF_4 + h\nu \rightarrow CF_4^* \rightarrow F_2^- + CF_x^+ + (2 - x)\,F \qquad (x \leq 2) \qquad (8)$$

The calculated enthalpies of reaction of (7) are 11.3, 17.5 and 20.6 eV for x = 3–1, respectively; for (8) they are 16.2 and 19.2 eV for x = 2–1, respectively. The F^- ion yield from reaction (7) recorded here is in good agreement with a previous study in the photon energy range 12–31 eV reported by Mitsuke *et al*.[25] The F^- and F_2^- yields are also in good agreement with those reported by Scully at higher resolution in the photon range 20–35 eV [(Ref. 31), Figures 3(c) and 3(d)], but *absolute* cross sections were not determined in this earlier work. It is immediately obvious from Figure 3 that the F^- and F_2^- yields share a similar feature between 20 and 23 eV. Mitsuke *et al*. assigned this feature in the F^- yield to three Rydberg transitions ($3t_2 \rightarrow npt_2$ n = 4, 5 and 6 at energies 20.96, 21.16 and 21.45 eV, respectively) converging on the third excited valence state of CF_4^+ ($\tilde{C}\,^2T_2$).[25] The Rydberg states excited at these energies would then couple to an ion pair state which dissociates to F^-, the corresponding cation, and any neutral fragments. The presence of Rydberg states in this energy region has also been observed in a high resolution threshold photoelectron study of CF_4 by Yencha *et al*.[42] Autoionizing structure is observed from 20.3 to 21.6 eV, preceding the onset of the $\tilde{C}\,^2T_2$ state of CF_4^+. This can be observed in the TPES (Figure 3) as a slight rise above the baseline in the same energy range. We therefore propose that Rydberg states converging to CF_4^+ $\tilde{C}\,^2T_2$ couple to ion pair states which dissociate to both F^- and F_2^-. At 21.8 eV the F^- cross section is *ca.* 30 times larger than that for F_2^-. This may reflect the degree of coupling between states and/or the steric disadvantage on forming an extra bond to produce F_2^-.

The highest outer-valence electronic state of CF_4^+ is the $\tilde{D}\,^2A_1$ state at 25.1 eV, whereas the next discrete state in the photoelectron spectrum corresponding to ionization of the $2t_2$ inner-valence electron is the $\tilde{E}\,^2T_2$ state at 40.3 eV.[33,43] Both the F^- and F_2^- yields increase above 25 eV, and the spectral features at higher

energies are more clearly observed in the work of Scully[31] which extends up to 110 eV. In particular, broad maxima in the F^- yield are observed at 29.4 and 33.5 eV [Figure 3(c)] which cannot be assigned to a simple one-electron valence-Rydberg excitation. The most likely explanation of these features is the result of promotion of outer-valence $4t_2$ and $3t_2$ electrons into shape resonance states. β-parameter measurements from angle resolved photoelectron spectroscopy[43] suggest that shape resonances in CF_4 do exist at energies 10–15 eV above the ionization energy of the outer-valence t_2 orbitals, and the two broad peaks observed here in the F^- dissociation channel are *ca.* 12 eV above their respective ionization energies. Although the signal-to-noise ratio is inferior, there is some evidence for a shape resonance in the F_2^- yield at 33.5 eV, but there is clearly no such resonance at 29.4 eV (Figure 3(d)). If this is indeed true, the absence at 29.4 eV, in contrast to its presence at 33.5 eV, may result from the different character of the $3t_2$ (C–F σ bonding) and $4t_2$ (F 2pπ non-bonding) orbitals,[33] or from different predissociation mechanisms. Shape resonances have also been observed in the F^- yield from SF_6.[26]

C. SF_5CF_3

The white light negative ion mass spectrum for SF_5CF_3 shows eight peaks corresponding to the anions F^- (100%), CF^- (1%), F_2^- (2%), SF^- (1%), SF_2^- (1%), SF_3^- (1%), SF_4^- (2%) and SF_5^- (14%). With the exception of SF_5^-, all of the anion signals increase linearly with pressure. SF_5^- formed following photoexcitation of SF_5CF_3 shows similar pressure behaviour to SF_5^- formation from SF_6, and is discussed in more detail in Section C. II.

C. I. Thermochemistry. Ion yields for the anions resulting from ion pair formation are presented in Figure 4, the data in Table I. The quantum yields are all in the range $10^{-7} – 10^{-4}$, consistent with those expected for a large polyatomic molecule.[21,22] All spectra were recorded with the higher-energy grating. The ion yield of F^- below 12 eV was also recorded with the lower-energy grating and LiF window to display the

threshold region more clearly, and an AE_{298} value of 11.05 ± 0.05 eV was determined. The following reactions are suggested as the main sources of formation of the anions:

$$SF_5CF_3 + h\nu \rightarrow SF_5CF_3^* \rightarrow F^- + CF_3^+ + SF_4 \quad (9)$$

$$SF_5CF_3 + h\nu \rightarrow SF_5CF_3^* \rightarrow SF_4^- + CF_3^+ + F \quad (10)$$

$$SF_5CF_3 + h\nu \rightarrow SF_5CF_3^* \rightarrow SF_3^- + CF_3^+ + F + F \quad (11)$$

$$SF_5CF_3 + h\nu \rightarrow SF_5CF_3^* \rightarrow F_2^- + CF_3^+ + SF_3 \quad (12)$$

$$SF_5CF_3 + h\nu \rightarrow SF_5CF_3^* \rightarrow SF_2^- + CF_3^+ + 3F \quad (13)$$

$$SF_5CF_3 + h\nu \rightarrow SF_5CF_3^* \rightarrow SF^- + CF_3^+ + 4F \quad (14)$$

In all cases the cation formed is CF_3^+, the associated anion therefore resulting from the SF_5 part of SF_5CF_3. This is reflected in the results; five different anions containing sulfur are detected compared to one containing carbon, CF^-, which was only just detected above the sensitivity limit of the apparatus. The S–C bond is most likely to be the weakest in the molecule, the 0 K dissociation energy measured as 3.86 ± 0.45 eV.[16] In addition, Xu *et al.* have calculated bond dissociation energies in SF_5CF_3, resulting in D_o (SF_5CF_2–F) > D_o (F–SF_4CF_3) > D_o (SF_5–CF_3).[44] We cannot say conclusively that reactions (9)–(14) are responsible for *all* of the detected anion signals. Certainly, more channels become energetically accessible at higher energies. It is, however, interesting that the thermochemical thresholds for reactions (9)–(14) approximately reflect the observed AE values (Table I). The only apparent exception is reaction (12), F_2^- production, where steric constraints on forming a new bond could be responsible. This trend can be visualized in Figure 4 by vertical arrows representing the enthalpies of the calculated thermochemical thresholds, within the approximations outlined in Section III. These values for $\Delta_r H^o_{298}$ are 11.6, 13.5, 15.4, 13.7, 20.6 and 23.2 eV for reactions (9)–(14), respectively. They were calculated using literature enthalpies of formation ($\Delta_f H^o_{298}$ in kJ mol^{-1}); SF_5CF_3 = –1717 (Ref. 38), F = +79 (Ref. 38), F^- = –249 (Refs. 38, 39), F_2^- = –301 (Ref. 40), CF_3^+

= +406 (Ref. 15), SF_4 = –763 (Ref. 38), SF_4^- = –908 (Refs. 38, 45), SF_3 = –503 (Ref. 38), SF_3^- = –802 (Refs. 38, 46), SF_2^- = –384 (Refs. 38, 45) and SF^- = –207 (Refs. 38, 47). No errors are given but there is significant uncertainty in some of these values, which probably explains why the calculated AE is sometimes greater than the experimental value (*e.g.* F^- and SF_4^- in Figure 4). The formation of F^- and F_2^- over the complete energy range 11–35 eV are unlikely to result exclusively from reactions (9) and (12) respectively, whereas the channels available to form the sulfur-containing anions are fewer. Indeed, the ion yields for F^- and F_2^- do show structure over a much wider energy range than those of SF_x^- (x = 1–4).

C. II. Yield of SF_5^-. The ion yields for F^-, F_2^- and SF_5^- are presented in Figure 5 and compared to the TPES of SF_5CF_3.[13] SF_5^- is the only anion detected which is *not* associated with ion pair formation. Three comparisons can be made between the behaviour of SF_5^- formed from SF_5CF_3 and SF_5^- formed from SF_6. First, the SF_5^- signal increases non-linearly with pressure, with the rate of change of signal increasing as the pressure increases. Second, electron attachment to SF_5CF_3 is dissociative forming SF_5^- (and CF_3) as the only significant channel.[8-12] Third, the ion yield of SF_5^- shows many similarities to the TPES of SF_5CF_3. We therefore propose that the dominant mechanism for the production of SF_5^- from SF_5CF_3 is dissociative electron attachment following photoionization as a source of low-energy electrons:

$$SF_5CF_3 + h\nu \rightarrow SF_5CF_3^+ + e^- \qquad (15)$$

$$SF_5CF_3 + e^- \rightarrow (SF_5CF_3^-)^* \rightarrow SF_5^- + CF_3 \qquad (16)$$

C. III. Discussion of the ion yields. As shown in Figure 5, the F^- and F_2^- ion yields also show similarities to the TPES of SF_5CF_3. Due to its higher signal-to-noise ratio, it is in the F^- spectrum where these similarities are most obvious. In the photon energy range 13–23 eV the agreement between peak positions is good and the relative signal strengths show only small differences. The resemblance of the F^-

ion yield to the TPES could be explained by a process involving electron attachment being significant in F^- formation. This has been the case in the discussion above, explaining the formation of SF_5^- from both SF_6 and SF_5CF_3. However, the F^- signal rises linearly with increasing gas pressure. This suggests strongly that a primary process, *i.e.* ion pair formation to $F^- + SF_4CF_3^+$ (or $F^- + CF_3^+ + SF_4$), is dominant.

For the purposes of this discussion the features in the F^- ion yield are labelled in figure 4(a). The experimental AE(F^-) is 11.05 eV, and this anion gives rise to peak 1 centred at 11.7 eV. This peak occurs below the onset of ionization for SF_5CF_3, reported as 12.9 eV,[13] so the presence of photoelectrons from reaction (15) is not relevant. The energy of peak 1 is close to peaks observed in the SF_5CF_3 photoabsorption[20] and total fluorescence yield[48] spectra at 11.4 eV. These two studies give different assignments to this transition. Holland *et al*.[20] assign it to a blend of several valence-valence transitions, whilst Ruiz *et al*.[48] assign it to a valence-Rydberg transition from the 29a' highest-occupied molecular orbital of SF_5CF_3 to a 4s Rydberg orbital. The contribution of fluorescence at this energy was reported to originate from the CF_3 fragment, following dissociation of $SF_5CF_3^*$ and production of an excited electronic state of the CF_3 radical. In addition, this was the most intense band observed within the photon energy range studied of 10–28 eV.[48] It must represent a transition to the same intermediate state which predissociates into states yielding both CF_3^* and F^- anions. We determine the ion pair quantum yield at the maximum of the peak in the F^- ion yield at 11.7 eV to be $\Phi = 1.5 \times 10^{-4}$. This small value, coupled with the fact that fluorescence from $SF_5CF_3^*$ is unlikely to have a large quantum yield, suggests strongly that predissociation into neutral fragments is the favoured process at this energy. A similar conclusion was reached by Shaw *et al*. in a comparable study of the dissociation dynamics of Rydberg states of some substituted methane molecules.[23] The agreement of peak positions in SF_5CF_3 between the photoabsorption spectrum,[20] the total fluorescence yield[48] and the F^- ion yield extends up to 17 eV, but above this energy similarities between the spectra are less clear.

It is interesting that the F^- ion pair quantum yield does not decrease above the onset of ionization of SF_5CF_3, 12.9 eV. Features 1 and 4 at 11.7 and 16.9 eV, for example, have $\Phi = 1.5 \times 10^{-4}$ and 3.4×10^{-4}, respectively (Table II). As a result of significant photoabsorption leading to ionization, one might expect the ion pair quantum yield to decrease, as observed for both SF_6 and CF_4 (Table II). However, above the ionization energy of SF_5CF_3 the F^- ion yield increases, approximately matching the shape of the TPES. In fact features 2–11 of Figure 4(a) occur at, or just below, vertical ionization energies in the TPES of SF_5CF_3.[20] Only feature 1 does not follow this trend. It seems unlikely that valence states of SF_5CF_3 which predissociate into ion pairs coincidentally lie very close to the ionization thresholds, certainly across this large energy range. It is much more likely that Rydberg states play an important role. Certainly the F^- ion yield would be explained if coupling to ion pair states was more significant from Rydberg states close to the ionization thresholds than from those lower in energy. Contributions to the F^- ion yield from low-lying Rydberg states would then be the dominant cause of peak 1, and very likely a weak background across the spectrum. F^- ions produced *via* high-lying Rydberg states would be dominant at higher energy, and hence responsible for features 2–11 in the ion yield. If this is true, it negates the generally accepted rule that it is low-*n*, and not high-*n*, Rydberg states which interact most strongly with ion-pair states. However, most of the ion-pair experiments on polyatomics to date have studied halogenated molecules where the lowest ion-pair threshold lies *below* the first ionisation energy,[21] so by definition it is the low-*n* states which have been the most widely studied. The difficulties in assigning peaks in the total fluorescence yield spectrum of SF_5CF_3 have already been noted by Ruiz *et al*.,[48] and at our modest resolution there are several valence-Rydberg transitions which could be assigned to peaks 2–11 in Figure 4(a). We simply comment that a much higher-resolution spectrum would be needed for such a large molecule in order to give definitive assignments.

An alternative mechanism than reaction (9) for production of F^- might be *via* dissociative electron attachment to SF_5CF_3,

e.g. $SF_5CF_3 + e^- \rightarrow (SF_5CF_3^-)^* \rightarrow F^- + SF_4 + CF_3$ (17)

We reject this because it is well known that the only product of low-energy electron attachment to SF_5CF_3 is SF_5^- (reaction (16)),[8-12] and we note the huge signal of the F^- ion yield to the relatively weak signal of SF_5^- (Figure 5). Furthermore, the only way that the F^- signal could show a linear dependence with pressure of SF_5CF_3 in these circumstances if, in addition, there was another reaction removing F^-,

e.g. $SF_5CF_3 + F^- \rightarrow SF_6^- + CF_3$ (18)

and the relative rate coefficient for reactions (16), (17) and (18) were 'correct'. We regard this as speculative and highly unlikely.

This analysis also extends to the ion yields for SF_4^-, SF_3^-, F_2^-, SF_2^-, and SF^-. The peak positions and the extent of structure observed for these anions can be explained in the same way as the F^- ion yield. The thermochemical considerations outlined in Section C. I. are also relevant. The SF_4^-, SF_3^-, and SF_2^- ion yields show less structure than is seen from F^-. In the energy regions where peaks are observed, their energies agree with those in the F^- ion yield, and hence with vertical ionization energies. We suggest the number of available ion pair states reflects the structure seen in the ion yields. SF_4^-, for example, is likely to arise from reaction (10) only. It is certainly the most sterically viable channel. Coupling of high-lying Rydberg states to this ion pair state will give rise to the peaks at 14 and 15 eV [Figure 4(b)]. Lack of structure above 16 eV represents the point where this ion pair state no longer couples significantly to Rydberg states. SF_3^- and SF_2^- also arise through coupling of high-lying Rydberg states to an appropriate ion pair state, and only over a limited energy range above the onset. In contrast, many more dissociation channels will be available to yield the anions F^- and F_2^-. As a result, structure in both ion yields extends extensively from onset up to 25 eV. Finally, it is noted that shape resonances have been observed in the

yields of many anions in both SF_6 and CF_4 above 25 eV.[26,31] There is no obvious evidence for such peaks in our ion yields from SF_5CF_3, but it would be surprising if they were not present.

V. CONCLUSIONS

The peaks in the F^- yields from both SF_6 and CF_4 have been assigned to Rydberg transitions,[24,25] and the assignments are not repeated here. However, there is some disagreement whether the transitions observed in the VUV absorption spectrum of SF_5CF_3,[6,20] and indeed the CF_3^* fluorescence excitation spectrum,[48] are due to intravalence or Rydberg transitions. Peaks in the absorption and electron energy loss spectra of SF_5CF_3 were assigned by Limao-Vieira *et al*.[6] to valence-Rydberg transitions, and quantum defects determined. Ruiz *et al*.[48] also assigned peaks in the absorption spectrum that led to CF_3 fluorescence to valence-Rydberg transitions. Holland *et al*.,[20] however, assigned the main peaks in the absorption spectrum to valence-valence transitions. Our spectra observe a different exit channel, *i.e.* photodissociation of excited states of SF_5CF_3 to production of anions. However, the primary excitation process in all these experiments is the same, and we favour their assignment to Rydberg transitions, for two reasons. First, all previous work on ion pair production from polyatomic molecules has preferred the process of Rydberg state photoexcitation, followed by predissociation into an ion pair state.[21,22] Second, apart from the low-energy peak in the F^- yield at 11.7 eV below the ionization energy of SF_5CF_3, all the F^- peaks have energies very close to peaks in the TPES of this molecule. Since it is Rydberg states that have energies converging on ground and excited electronic states of $SF_5CF_3^+$, it seems very likely that these F^- peaks correspond to photoexcitation of Rydberg states.

A summary of the numerical information obtained from the ion yields from SF_6, CF_4 and SF_5CF_3 is given in Table I, listing AEs of anions, cross sections and quantum yields. The anions observed from SF_5CF_3 were all seen in either the SF_6 or CF_4 study. The signal strengths from the SF_x^- anions, however, were marginally stronger from SF_5CF_3 than from SF_6, allowing their ion yields to be recorded. Unsurprisingly, F^- and F_2^- were observed from all three molecules. The most prominent features in the F^- ion yields from SF_6 and CF_4

occur below the onset of ionization. This is not the case for F^- from SF_5CF_3. This observation is clearly demonstrated in Table II when comparing the ion pair quantum yields of F^- above and below the onset of ionization for these three molecules.

ACKNOWLEDGEMENTS

We thank Dr David Shaw for help in running these experiments on beamline 3.1 of the SRS, Dr Michael Parkes for help with data collection and a critical reading of the manuscript, and Dr David Holland for providing absolute cross section data for SF_6 and SF_5CF_3. This collaboration between the groups in Birmingham and Belfast was partially funded by EPSRC Network grant GR/N26234/01. CCLRC is thanked for the provision of synchrotron beamtime.

[1] W. T. Sturges, T. J. Wallington, M. D. Hurley, K. P. Shine, K. Sihra, A. Engel, D. E. Oram, S. A. Penkett, R. Mulvaney and C. A. M. Brenninkmeijer, Science **289**, 611 (2000).

[2] R. Y. L. Chim, R. A. Kennedy and R. P. Tuckett, Chem. Phys. Lett. **367**, 697 (2003).

[3] P. A. Kendall, N. J. Mason, G. A. Buchanan, G. Marston, P. Tegeder, A. Dawes, S. Eden, P. Limao-Vieira and D. A. Newnham, Chem. Phys. **287**, 137 (2003).

[4] P. A. Kendall and N. J. Mason, J. Elec. Spec. Rel. Phen. **120**, 27 (2001).

[5] O. J. Nielsen, F. M. Nicolaisen, C. Bacher, M. D. Hurley, T. J. Wallington and K. P. Shine, Atmos. Environ. **36**, 1237 (2002).

[6] P. Limao-Vieira, S. Eden, P. A. Kendall, N. J. Mason, A. Giuliani, J. Heinesch, M. J. Hubin-Franskin, J. Delwiche and S. V. Hoffmann, Int. J. Mass Spec. **233**, 335 (2004).

[7] L. Huang, L. Zhu, X. Pan, J. Zhang, B. Ouyang and H. Hou, Atmos. Environ. **39**, 1641 (2005).

[8] R. A. Kennedy and C. A. Mayhew, Int. J. Mass Spec. **206**, AR1 (2001).

[9] W. Sailer, H. Drexel, A. Pelc, V. Grill, N. J. Mason, E. Illenberger, J. D. Skalny, T. Mikoviny, P. Scheier and T. D. Märk, Chem. Phys. Lett. **351**, 71 (2002).

[10] T. M. Miller, S. T. Arnold, A. A. Viggiano and W. B. Knighton, J. Chem. Phys. **116**, 6021 (2002).

[11] C. A. Mayhew, A. D. J. Critchley, D. C. Howse, V. Mikhailov and M. A. Parkes, Eur. Phys. J. D **35**, 307 (2005).

[12] H. Hotop, private communication (2007).

[13] R. Y. L. Chim, R. A. Kennedy, R. P. Tuckett, W. Zhou, G. K. Jarvis, D. J. Collins and P. A. Hatherly, J. Phys. Chem. A **105**, 8403 (2001).

[14] R. Y. L. Chim, R. A. Kennedy, R. P. Tuckett, W. Zhou, G. K. Jarvis, C. A. Mayhew, D. J. Collins and P. A. Hatherly, Surf. Rev. Lett. **9**, 129 (2002).

[15] G. A. Garcia, P. M. Guyon and I. Powis, J. Phys. Chem. A **105**, 8296 (2001).

[16] R. P. Tuckett, Adv. Fluorine Sci. (Elsevier) **1**, 89 (2006).

[17] C. Atterbury, R. A. Kennedy, C. A. Mayhew and R. P. Tuckett, Phys. Chem. Chem. Phys. **3**, 1949 (2001).

[18] C. Atterbury, A. D. J. Critchley, R. A. Kennedy, C. A. Mayhew and R. P. Tuckett, Phys. Chem. Chem. Phys. **4**, 2206 (2002).

[19] S. T. Arnold, T. M. Miller, A. A. Viggiano and C. A. Mayhew, Int. J. Mass Spec. **223**, 403 (2003).

[20] D. M. P. Holland, D. A. Shaw, I. C. Walker, I. J. McEwen, E. Apra and M. F. Guest, J. Phys. B: At. Mol. Opt. Phys. **38**, 2047 (2005).

[21] J. Berkowitz in U. Becker and D. A. Shirley (Eds.), *VUV and Soft X-Ray Photoionisation* (Plenum Press, New York, p263, 1996).

[22] A. G. Suits and J. W. Hepburn, Ann. Rev. Phys. Chem. **57**, 431 (2006).

[23] D. A. Shaw, D. M. P. Holland and I. C. Walker, J. Phys. B: At. Mol. Opt. Phys. **39**, 3549 (2006).

[24] K. Mitsuke, S. Suzuki, T. Imamura and I. Koyano, J. Chem. Phys. **93**, 8717 (1990).

[25] K. Mitsuke, S. Suzuki, T. Imamura and I. Koyano, J. Chem. Phys. **95**, 2398 (1991).

[26] S. W. J. Scully, R. A. Mackie, R. Browning, K. F. Dunn and C. J. Latimer, J. Phys. B: At. Mol. Opt. Phys. **35**, 2703 (2002).

[27] C. R. Howle, S. Ali, R. P. Tuckett, D. A. Shaw and J. B. West, Nucl. Instr. Meth. Phys. Res. B **237**, 656 (2005).

[28] C. A. Hunniford, S. W. J. Scully, K. F. Dunn and C. J. Latimer, J. Phys. B: At. Mol. Opt. Phys. **40**, 1225 (2007).

[29] NIST website, webbook.nist.gov/chemistry/

[30] P. M. Dehmer and W. A. Chupka, J. Chem. Phys. **62**, 4525 (1975).

[31] S. W. J. Scully, *PhD thesis* (Queen's University Belfast 2004).

[32] J. C. Traeger and R. G. McLoughlin, J. Am. Chem. Soc. **103**, 3647 (1981).

[33] J. C. Creasey, H. M. Jones, D. M. Smith, R. P. Tuckett, P. A. Hatherly, K. Codling and I. Powis, Chem. Phys. **174**, 441 (1993).

[34] A. J. Yencha, D. B. Thompson, A. J. Cormack, D. R. Cooper, M. Zubek, P. Bolognesi and G. C. King, Chem. Phys. **216**, 227 (1997).

[35] D. M. P. Holland, D. A. Shaw, A. Hopkirk, M. A. MacDonald and S. M. McSweeney, J. Phys. B: At. Mol. Opt. Phys. **25**, 4823 (1992).

[36] L. G. Christophorou and J. K. Olthoff, J. Phys. Chem. Ref. Data **29**, 267 (2000).

[37] M. A. Parkes, *PhD thesis* (University of Birmingham 2007).

[38] M. W. Chase, J. Phys. Chem. Ref. Data, Monograph no. 9 (1998).

[39] C. Blondel, C. Delsart and F. Goldfarb, J. Phys. B: At. Mol. Opt. Phys. **34**, L281 (2001).

[40] A. Artau, K. E. Nizzi, B. T. Hill, L. S. Sunderlin and P. G. Wenthold, J. Am. Chem. Soc. **122**, 10667 (2000).

[41] R. Y. L. Chim, C. Cicman, T. D. Märk, C. A. Mayhew, P. Scheier and R. P. Tuckett, Int. J. Mass Spectrom. **261**, 208 (2007).

[42] A. J. Yencha, A. Hopkirk, A. Hiraya, G. Dujardin, A. Kvaran, L. Hellner, M. J. Besnard-Ramage, R. J. Donovan, J. G. Goode, R. R. J. Maier, G. C. King and S. Spyrou, J. Elec. Spec. Rel. Phen. **70**, 29 (1994).

[43] D. M. P. Holland, A. W. Potts, A. B. Trofimov, J. Breidbach, J. Schirmer, R. Feifel, T. Richter, K. Godehusen, M. Martins, A. Tutay, M. Yalcinkaya, M. Al-Hada, S. Eriksson and L. Karlsson, Chem. Phys. **308**, 43 (2005).

[44] W. Xu, C. Xiao, Q. Li, Y. Xie and H. F. Schaefer, Mol. Phys. **102**, 1415 (2004).

[45] A. E. S. Miller, T. M. Miller, A. A. Viggiano, R. A. Morris, J. M. Van Doren, S. T. Arnold and J. F. Paulson, J. Chem. Phys. **102**, 8865 (1995).

[46] R. N. Compton, P. W. Reinhardt and C. D. Cooper, J. Chem. Phys. **68**, 2023 (1978).

[47] M. L. Polak, M. K. Gilles and W. C. Lineberger, J. Chem. Phys. **96**, 7191 (1992).

[48] J. A. Ruiz, A. Kivimäki, M. Stankiewicz, E. M. Garcia, M. Coreno, S. Ali, J. Koperski, E. Rachlew, G. Serrano, V. Feyer and R. P. Tuckett, Phys. Chem. Chem. Phys. **8**, 5199 (2006).

Table I. Appearance energies, cross sections, and quantum yields for anions observed from photoexcitation of SF_6, CF_4 and SF_5CF_3 in the range 10–30 eV.

Molecule [AIE [a] (eV)]	Anion	AE [b] (eV)	Cross section maximum [c] (cm^2)	Energy [d] (eV)	Quantum Yield [e]
SF_6 [15.1]	F^-	12.7	7.1×10^{-21}	14.2	2.4×10^{-4}
	F_2^-	16.3	8.7×10^{-23}	18.3	1.2×10^{-6}
	SF_5^-	15.1	–[f]	17.5	–[g]
	SF_6^-	15.1	–[f]	17.1	–[g]
CF_4 [15.4]	F^-	13.0	1.4×10^{-21}	14.0	2.8×10^{-5}
	F_2^-	20.1	2.5×10^{-23}	21.6	3.5×10^{-7}
SF_5CF_3 [12.9]	F^-	11.05	3.4×10^{-20}	16.9	3.4×10^{-4}
	F_2^-	16.1	7.4×10^{-22}	17.9	7.1×10^{-6}
	SF^-	24.0	1.4×10^{-22}	28.8	1.2×10^{-6}
	SF_2^-	20.2	1.4×10^{-22}	24.2	8.8×10^{-7}
	SF_3^-	15.4	2.9×10^{-21}	17.6	2.8×10^{-5}
	SF_4^-	13.0	2.9×10^{-21}	14.1	3.7×10^{-5}
	SF_5^-	13.0	–[f]	17.0	–[g]

[a] Adiabatic ionization energy. Values are taken from the observed onset of ionization for SF_6 (Ref. 34), CF_4 (Ref. 33) and SF_5CF_3 (Ref. 13).

[b] Observed appearance energy (AE) from this work. We estimate the error to be ± 0.2 eV, based on the resolution and step size used when recording ion yields.

[c] Cross section for anion production following photoexcitation of the parent molecule.

[d] Energy of strongest peak. It is at this energy, where appropriate, where cross section and quantum yield measurements are taken.

[e] Quantum yields for anion production, obtained by dividing cross sections for anions (column 4) by total photoabsorption cross sections. The latter values are given for SF_6, CF_4 and SF_5CF_3 in Refs. 35, 2 and 20, respectively.

[f] Normalization of the signal strength to determine an effective cross section is not possible because of the non-linear dependence of signal with pressure.

[g] Quantum yield cannot be determined because the cross section is not defined.

Table II. F^- ion pair quantum yields (Φ_F-) at energies below and above the onsets of ionization for SF_6, CF_4 and SF_5CF_3. Cross sections from this work are normalized to photoabsorption cross sections for SF_6 (Ref. 35), CF_4 (Ref. 2) and SF_5CF_3 (Ref. 20) to give values for Φ_F-.

Molecule	Φ_F- below onset of ionization	Φ_F- above onset of ionization
SF_6	2.4×10^{-4} at 14.2 eV	1.5×10^{-5} at 24.6 eV
CF_4	2.8×10^{-5} at 14.0 eV	9.3×10^{-6} at 21.8 eV
SF_5CF_3	1.5×10^{-4} at 11.7 eV	3.4×10^{-4} at 16.9 eV

Figure Captions

Figure 1 Cross sections for anion production following photoexcitation of SF_6. Note that the SF_5^- and SF_6^- spectra are not on an absolute scale. Ion yields were recorded as a function of photon energy between 12 and 35 eV with a step size of 0.1 eV and a wavelength resolution of 6 Å. This resolution is equivalent to 0.07 eV at 12 eV, 0.6 eV at 35 eV. The ion yields are compared with the threshold photoelectron spectrum of SF_6 (Ref. 33).

Figure 2 Pressure dependence of F^- and SF_5^- anion signals from SF_6.

Figure 3 Cross sections for anion production following photoexcitation of CF_4. (a) and (b) F^- and F_2^- ion yields recorded as a function of photon energy between 12 and 35 eV with a step size of 0.1 eV and a wavelength resolution of 6 Å (this work). This resolution is equivalent to 0.07 eV at 12 eV, 0.6 eV at 35 eV. The cross sections are on an absolute scale. (c) and (d) F^- and F_2^- ion yields from Scully (Ref. 31) recorded over a narrower energy range at a higher resolution of 0.5 and 2.0 Å, respectively. The cross sections are now on a relative scale. (e) Threshold photoelectron spectrum of CF_4 for comparison (Ref. 33).

Figure 4 Cross sections for anion production following photoexcitation of SF_5CF_3. Ion yields were recorded as a function of photon energy between 10.5 and 35.0 eV with a step size of 0.1 eV and a wavelength resolution of 6 Å. This resolution is equivalent to 0.05 eV at 10.5 eV, 0.6 eV at 35 eV. Note that the F^- spectrum below 12 eV was recorded with the lower-energy grating, and the data spliced into the higher-energy spectrum. Solid arrows in the F^- through SF^- yields show energies of the thermochemical thresholds calculated for reactions (9)–(14), respectively.

Figure 5 Cross sections for anion production following photoexcitation of SF_5CF_3. Note that the SF_5^- spectrum is not on an absolute scale. Ion yields were recorded as a function of photon energy between 10.5 and 35.0 eV with a step size of 0.1 eV and a wavelength resolution of 6 Å. This resolution is equivalent to 0.05 eV at 10.5 eV, 0.6 eV at 35 eV. The ion yields are compared with the threshold photoelectron spectrum of SF_5CF_3 (Ref. 13).

Figure 1

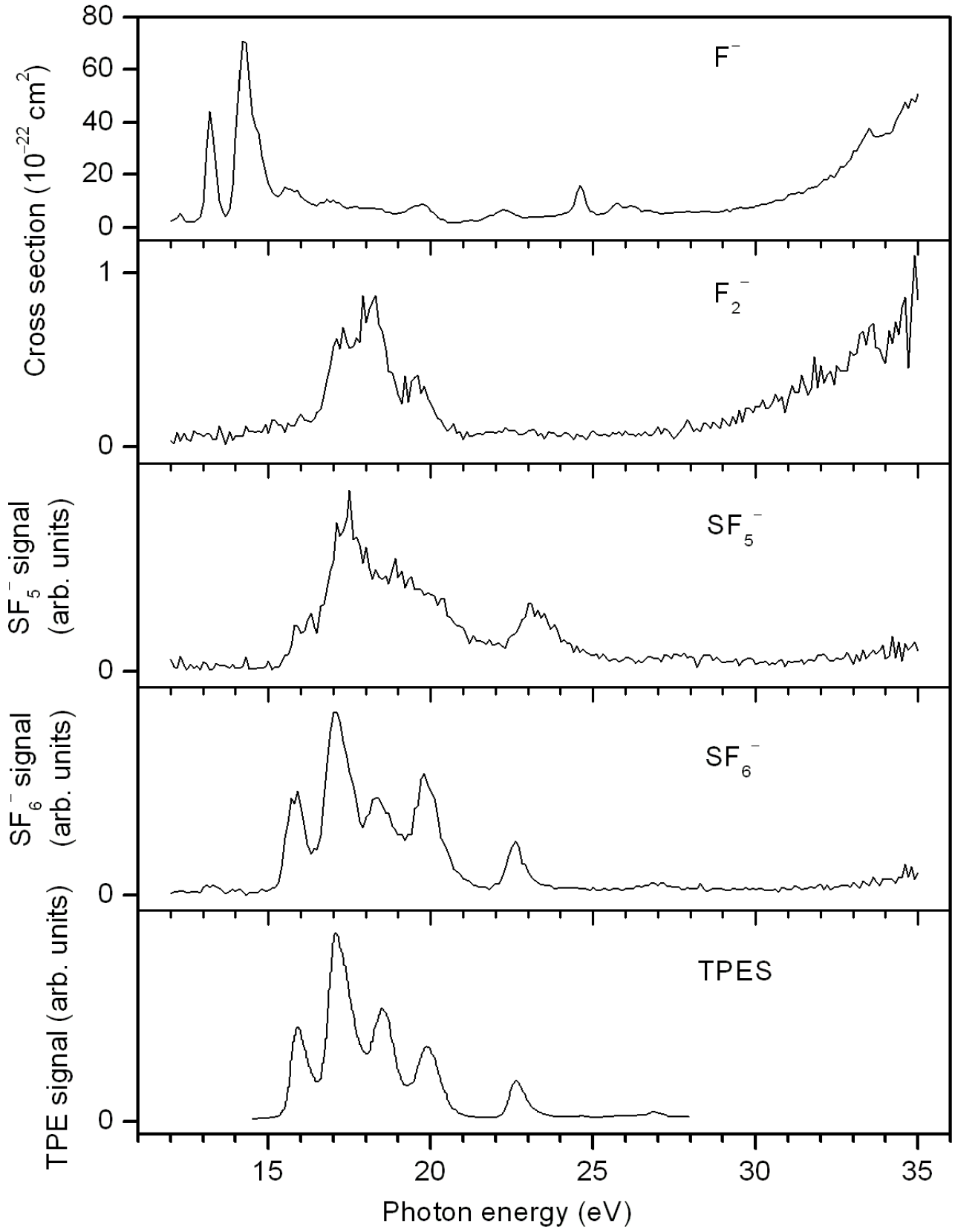
Cross section (10^{-22} cm^2)
80
60
40
20
0
F^-
1
0
F_2^-
SF_5^- signal (arb. units)
0
SF_5^-
SF_6^- signal (arb. units)
0
SF_6^-
TPE signal (arb. units)
0
TPES
15
20
25
30
35
Photon energy (eV)

Figure 2

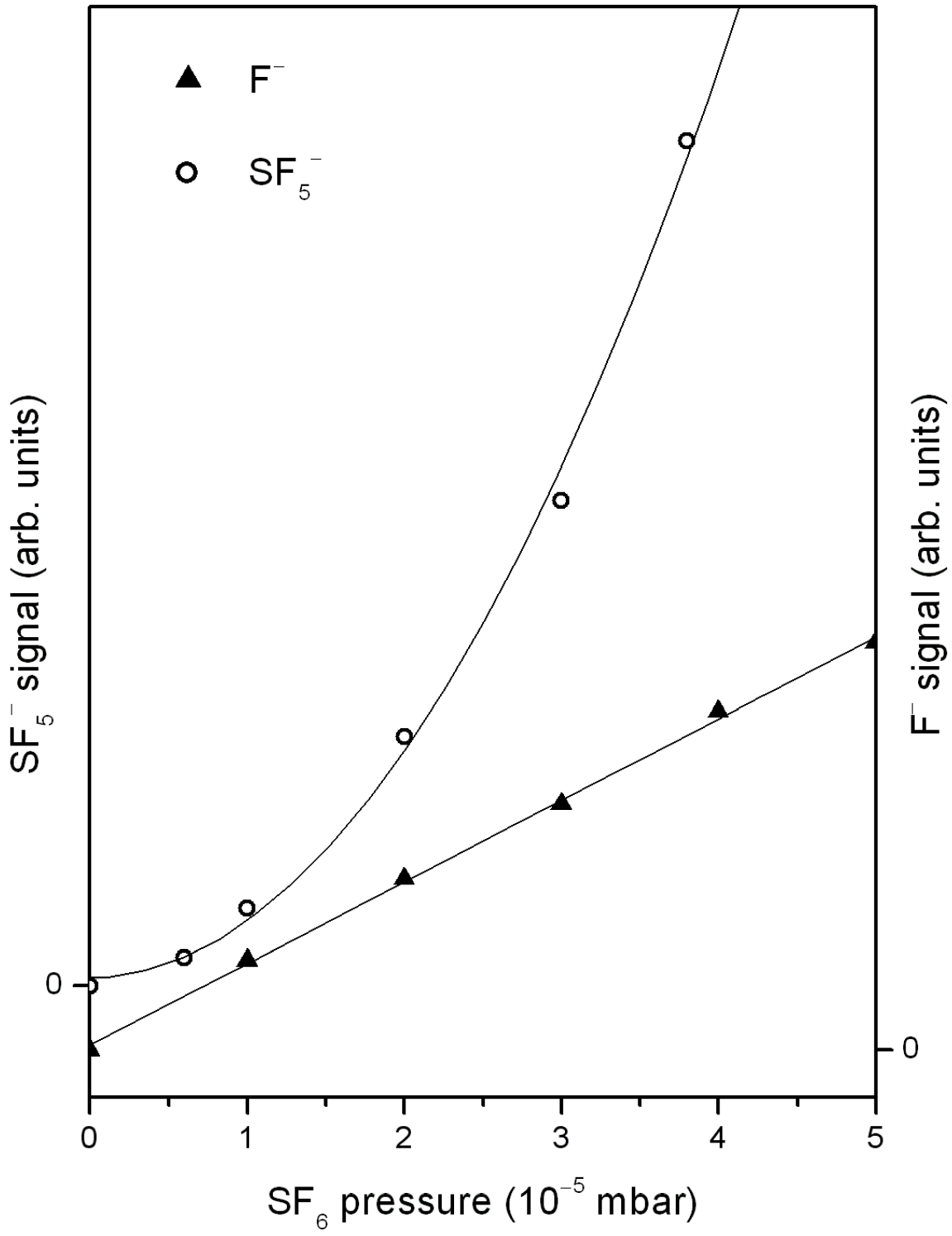
F⁻
SF5⁻
SF5⁻ signal (arb. units)
F⁻ signal (arb. units)
0
0
0
1
2
3
4
5
SF6 pressure (10⁻⁵ mbar)

Figure 3

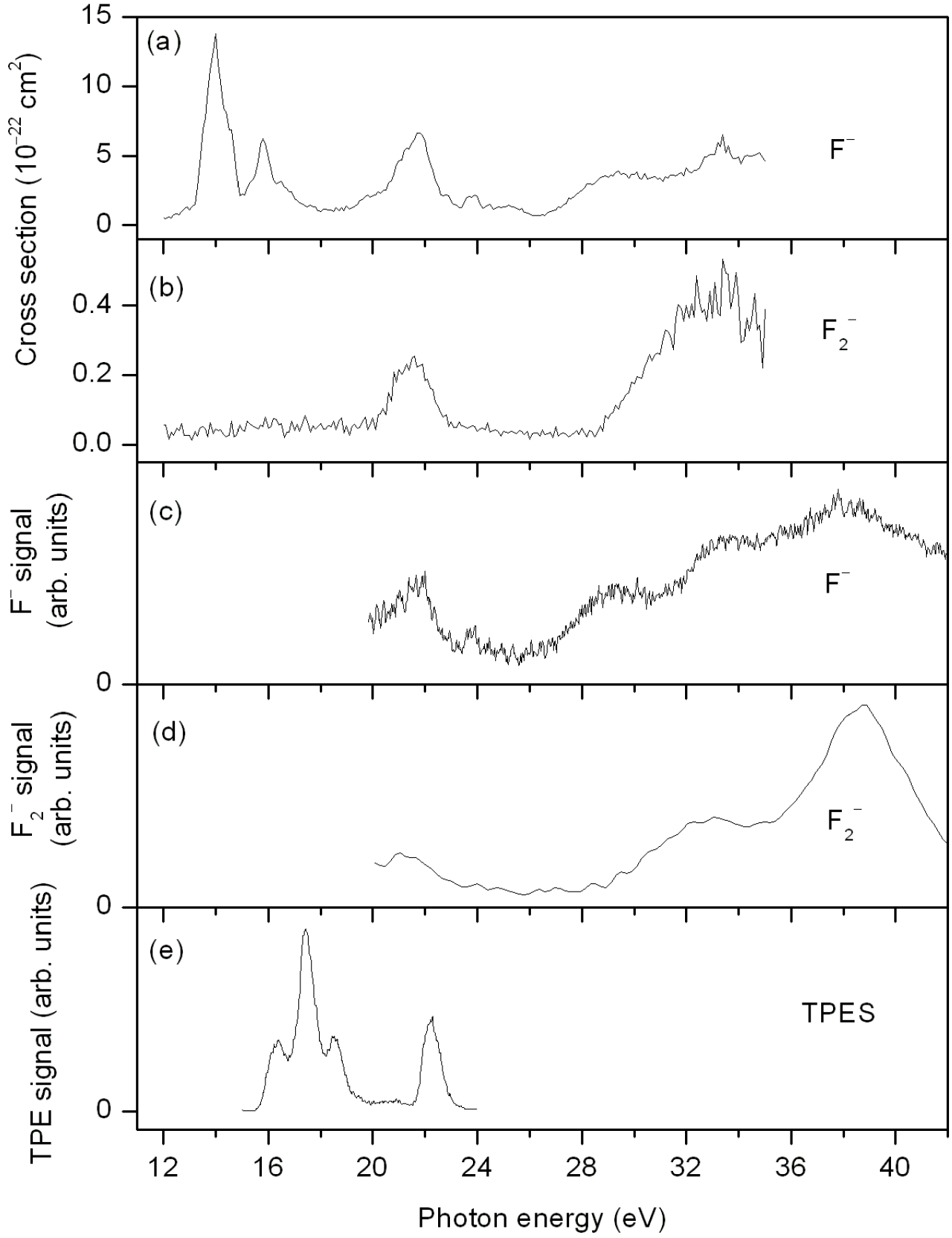
(a)
(b)
(c)
(d)
(e)
F⁻
F₂⁻
F⁻
F₂⁻
TPES
Cross section (10⁻²² cm²)
F⁻ signal (arb. units)
F₂⁻ signal (arb. units)
TPE signal (arb. units)
Photon energy (eV)
15
10
5
0
0.4
0.2
0.0
12
16
20
24
28
32
36
40

Figure 4

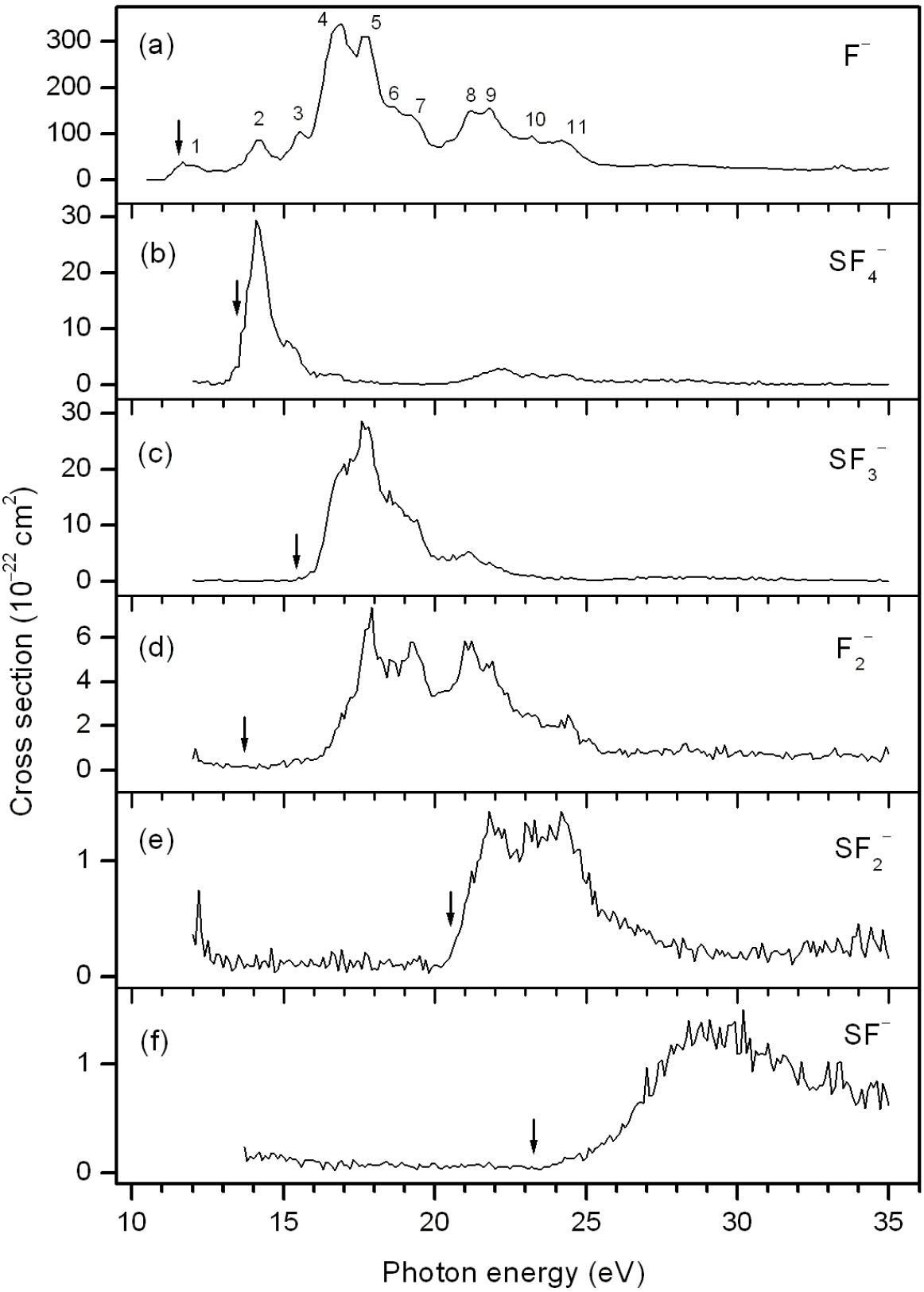
(a)
F⁻
(b)
SF4⁻
(c)
SF3⁻
(d)
F2⁻
(e)
SF2⁻
(f)
SF⁻
1
2
3
4
5
6
7
8 9
10
11
Cross section (10⁻²² cm²)
Photon energy (eV)

Figure 5

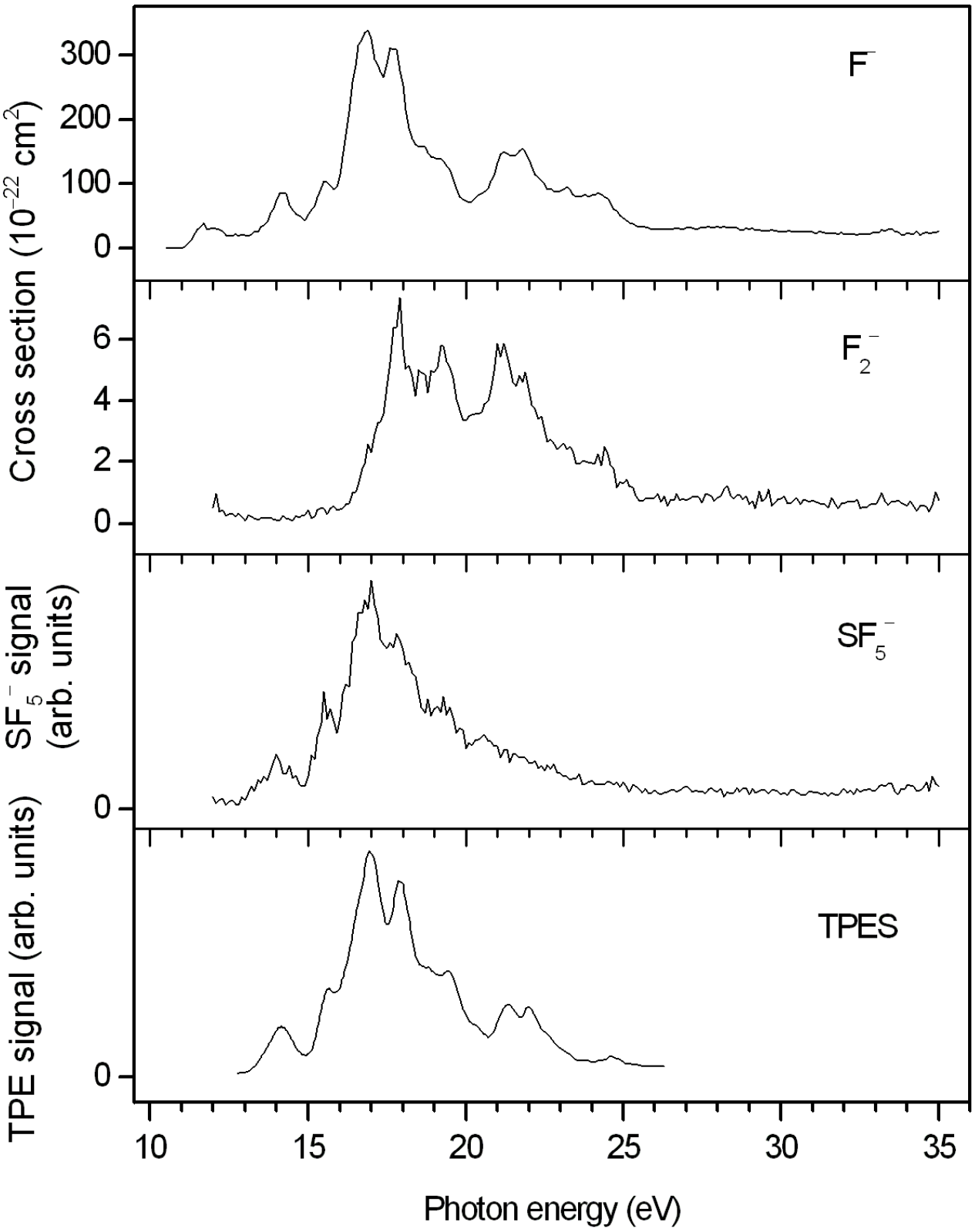
F⁻
F₂⁻
SF₅⁻
TPES
Cross section (10⁻²² cm²)
SF₅⁻ signal (arb. units)
TPE signal (arb. units)
Photon energy (eV)
300
200
100
0
6
4
2
0
0
0
10
15
20
25
30
35